

Hitchhiker's guide to second-generation Car-Parrinello ab-initio molecular dynamics

Thomas D. Kühne*

Center for Advanced Systems Understanding (CASUS),

Helmholtz Zentrum Dresden-Rossendorf, Germany and

Institute of Artificial Intelligence, Technische Universität Dresden, Germany

(Dated: January 21, 2026)

In a recent letter [T. D. Kühne, M. Krack, F. Mohamed and M. Parrinello, Phys. Rev. Lett. **98**, 066401 (2007)], we outlined a new Car-Parrinello-like approach to Born-Oppenheimer molecular dynamics. Here, we provide a guide to performing actual calculations using our method and demonstrate this on liquid water at ambient conditions. We do not go into methodological details beyond those necessary for applying this approach, but focus on practical details pertinent to our particular implementation within the CP2K/QUICKSTEP code [T. D. Kühne et al., J. Chem. Phys. **152**, 194103 (2020)].

PACS numbers: 31.15.-p, 31.15.Ew, 71.15.-m, 71.15.Pd

I. INTRODUCTION

Molecular dynamics^{1,2} (MD) methods are used to extract static and dynamic equilibrium properties. Therefore, before starting any MD simulation, one must be convinced that one is starting from an equilibrated system. This may sound trivial, but please keep in mind that within the second-generation Car-Parrinello (CP2G) *ab initio* MD (AIMD) method^{3–5}, the Hamiltonian is built-up solely using the propagated one-particle density matrix (DM). Although in the end, this should be a good approximation to the ground state of self-consistent Kohn-Sham (KS) density functional theory (DFT)^{6,7}, this will probably not be valid from the outset and will never be fully exact. It is therefore essential to perform the final equilibration using the fixed DM propagation (DMP) parameters, and we will explain shortly how this is done.

It is advisable to first perform a short pre-equilibration at the DFT level with a conventional Born-Oppenheimer MD (BOMD)^{4,8} simulation using either a massive Nosé-Hoover^{9,10}, high-friction (for the particular integrator of Ricci and Ciccotti¹¹ around $1/20 \geq \gamma \times dt \gg 1/1000$) Langevin, or the recently developed Bussi-Parrinello¹² thermostat.

To demonstrate how to conduct CP2G AIMD simulations using the CP2K/QUICKSTEP code¹³, we start with our ubiquitous 32 liquid water system at ambient conditions (T=300 K, P=1 bar, a=9.8528 Å)¹⁴. Specifically, we will use the geometry of /CP2K/TESTS/QS/BENCHMARK/H2O-32.INP, which has been equilibrated using the TIP5P force field¹⁵. The employed Goedecker-Teter-Hutter (GTH) pseudopotentials^{16–18}, as well as the corresponding Gaussian-type basis-sets, are provided in the appendix. The example for instruction is somewhat crude. We tried our best at a judicious trade-off between accuracy and speed, so do not forget that a more complete basis set may be necessary for a publication-quality simulation.

II. PART 0: BORN-OPPENHEIMER MOLECULAR DYNAMICS-BASED PRE-EQUILIBRATION

The initial BOMD reads as follows (please consult the online manual at <https://manual.cp2k.org> for details).

```
&FORCE_EVAL
  METHOD QS
  &DFT
    BASIS_SET_FILE_NAME ./H2O.qbs
    POTENTIAL_FILE_NAME ./GTH_POTENTIALS
    &MGRID
      CUTOFF 240
    &END MGRID
    &QS
      EPS_DEFAULT 1.0E-12
      EXTRAPOLATION ASPC
      EXTRAPOLATION_ORDER 3
      MAP_CONSISTENT TRUE
    &END QS
    &SCF
      EPS_SCF 5.0E-7
      MAX_SCF 25
      &OT ON
        MINIMIZER DIIS
        STEPSIZE 0.15
      &END OT
    &OUTER_SCF
      EPS_SCF 5.0E-7
      MAX_SCF 40
    &END OUTER_SCF
    SCF_GUESS RESTART
    #MAX_SCF_HISTORY 1
    &PRINT
      &RESTART_HISTORY
        EACH 1 1 0
        FILENAME =RESTART
        BACKUP_COPIES 5
      &END RESTART_HISTORY
    &END PRINT
  &END SCF
```

```

&XC
  &XC_FUNCTIONAL PBE
  &END XC_FUNCTIONAL
&END XC
&END DFT
&SUBSYS
  &CELL
    ABC 9.8528 9.8528 9.8528
    UNIT ANGSTROM
  &END CELL
# 32 H2O (TIP5P,1bar,300K) a = 9.8528
&COORD
  &END COORD
&KIND H
  BASIS_SET DZVP-GTH
  POTENTIAL GTH-PBE-q1
&END KIND
&KIND O
  BASIS_SET DZVP-GTH
  POTENTIAL GTH-PBE-q6
&END KIND
&TOPOLOGY
  CONNECTIVITY OFF
  &END TOPOLOGY
  &END SUBSYS
&END FORCE_EVAL
&GLOBAL
  PROJECT H2O-32
  RUN_TYPE MD
  PRINT_LEVEL LOW
  WALLTIME 28000
&END GLOBAL
&MOTION
  &MD
    ENSEMBLE NVT
    STEPS 10000
    TIMESTEP 0.5
    TEMPERATURE 300.0
    &THERMOSTAT
      TYPE NOSE
      REGION MASSIVE
      &NOSE
        LENGTH 3
        YOSHIDA 3
        TIMECON 100.0
        MTS 2
      &END NOSE
    &END THERMOSTAT
  &END MD
  &END MOTION
  &EXT_RESTART
    RESTART_FILE_NAME H2O-32-1.restart
  &END EXT_RESTART

```

There are a few subtleties concerning the `RESTART_HISTORY`. Above all, one must ensure that sufficient previous DMs are stored. Also, using `EXTRAPOLATION ASPC` causes `BACKUP_COPIES` to always be `EXTRAPOLATION_ORDER + 2`. Furthermore, with `EACH`

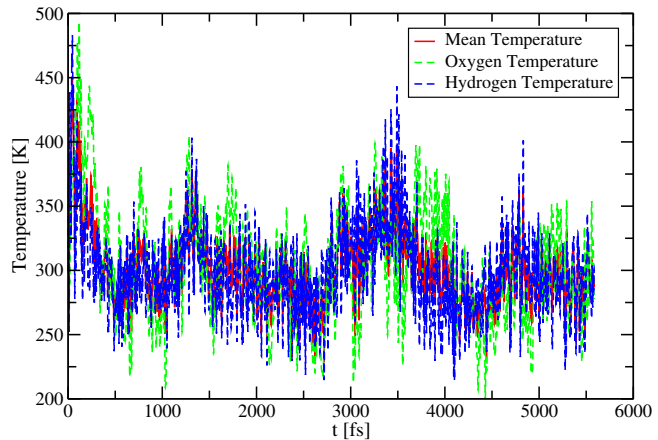


FIG. 1: Nuclear temperature as a function of time during the BOMD-based pre-equilibration.

1 1 0, it is ensured that the DM is only stored after whole AIMD steps, and during the self-consistent field (SCF) cycle. At this stage, the evolution of nuclear temperature over time resembles Fig. 1. Since we are still in the pre-equilibration phase, this is good enough to proceed. Whenever the initial structure is already sufficiently equilibrated at the DFT level, this step can simply be omitted.

III. PART I: OPTIMIZING THE DENSITY MATRIX PROPAGATION

We are now in a position to start with the actual parameter optimization, which consists of two independent parts: (i) the DMP optimization to approach the BO surface as closely as possible and (ii) the adjustment of the modified Langevin equation, which will be described in detail in section IV. One should mention that the first part is system-dependent and determines the eventual accuracy of the resulting potential energy surface and, more importantly, the associated nuclear forces, whereas the modified Langevin equation is responsible for the correct sampling of the Boltzmann distribution.

The optimization of the DMP itself consists of two small subtasks: (ia) the determination of the best corrector step size, and (ib) the identification of the optimal order K of the always-stable predictor corrector (ASPC) integrator^{19,20}. The `EXTRAPOLATION_ORDER k` within CP2K is equivalent to $K + 2$. These subproblems are independent from each other, so only four parameters in total need to be individually determined, or only two if only interested in static equilibrium properties.

A. Identification of the Best Corrector Step Size

One might ask whether this is not superfluous, as this step size should be equivalent to ω of Ref. [3]. Unfor-

tunately (or fortunately, from a methodological perspective), life is not that easy due to the particular choice of the corrector used in CP2K/QUICKSTEP.

Briefly for the experts, ω is only valid within the original Grassmann manifold of idempotent DMs²¹, or equivalently, orthonormal KS orbitals. In the original Car-Parrinello (CPMD) approach²², this is enforced by a holonomic constraint that has to be fulfilled at every step. Time-steps up to the resonance limit can additionally be used. The use of an idempotency conserving direct minimizer, such as the orbital transformation²³ (OT) method, is mainly responsible for the favorable computational cost of AIMD in comparison to CPMD. When using OT, which was inspired by the exponential transformation method²⁴, the orbitals are parameterized by an auxiliary variable. Geometrically, this corresponds to an auxiliary tangent space (which is a linear space) in which the minimization is performed. In this way, the idempotency constraint is always fulfilled – even in an incomplete minimization! However, this is only the beginning of the story, as a preconditioner²⁵ is still to be applied. The rationale for our method is the knowledge that the exact inverse Hessian matrix allows us to find the minimum in one step whenever the objective function is a quadratic function. Usually, the objective function is not quadratic but is assumed to be nearly quadratic near the minimum. Using OT, the objective function is exactly quadratic with respect to the introduced auxiliary variable. We, therefore, try to approach the exact minimum by using as good a preconditioner as possible.

Long story short, these transformations are very implementation-dependent, but they also need to be, at least in principle, applied to ω . When done explicitly, this results in ω' . This value is far from optimal, since ω is merely the easiest non-trivial solution for which all roots of the characteristic equation of the recurrence formula for the error propagation lie within the complex unit circle. Thus, ω can easily be optimized without destroying the always-stable property.

As a consequence – and this is important, so we ask the non-experts to tune back in – only *approximate* eigenfunctions are obtained, which causes a slight error in the forces. In comparison to the dissipation due to the non-symplecticity of the Gear-type predictor-corrector integrator²⁶, this is negligible. Nevertheless, it is corrected by the modified Langevin equation, as described in section V.

Theory aside, it is actually ω' that corresponds to STEPSIZE within the OT section of CP2K/QUICKSTEP, and it is 0.15 by default. From experience, the optimal value is somewhat lower and lies between 0.05 and 0.15. In order to bracket the optimal value, a few very short exploration runs are performed. Typically, 3 to 7 exploration runs of a few hundred steps are sufficient (check that the OT convergence criterion has stabilized!). The goal is not so much to squeeze out the best STEPSIZE value, but to ensure that the propagation does not break down. Naturally, one starts these exploration runs in

separate directories by restarting the previous relaxation runs. For this purpose, as the careful reader has recognized, we have been performing our BOMD relaxation with `RESTART_HISTORY` enabled in order to store not only the last but all previous DMs. By activating `SCF_GUESS HISTORY_RESTART` and the usual `EXT_RESTART`, a clean restart is performed, which reads in all necessary DMs and predicts the first DM to calculate the first force needed to get into the velocity Verlet loop. The corrector for this initial step is always applied only once (if `MAX_SCF_HISTORY > 1`, make sure that the last MD step of the previous run has properly finished!) and is discarded. Think it through, since whenever the last MD step of the previous run has properly finished, this is the desired consistent restart. After this initial half-step, all subsequent MD steps can be performed with as many corrector steps as desired.

At this point, our method needs to be activated by choosing `(EXTRAPOLATION ASPC)` and setting `EXTRAPOLATION_ORDER` to any arbitrary, but sufficiently low value. For the beginning, we recommend 0 or 1. Such a choice will cause the energy loss to be somewhat higher, but that is not important in our current situation. What matters is the comparison between different choices of `STEPSIZE`, keeping all other parameters fixed. Furthermore, the number of corrector steps needs to be determined by `MAX_SCF_HISTORY`. In this way, the deviation from the BO surface can be systematically controlled. It depends on the particular system and the accuracy demands, but we have shown on a variety of systems that values between 1 and 2 normally suffice, even for notoriously difficult systems.

Finally, the `ENSEMBLE` needs to be changed to `NVE` so that the relevant dissipation of total energy can be monitored. In summary, our previous input needs to be modified as follows.

```

&DFT
  RESTART_FILE_NAME RESTART
  &QS
    EXTRAPOLATION ASPC
    EXTRAPOLATION_ORDER 3
  &END QS
  &SCF
    &OT ON
      MINIMIZER DIIS
      STEPSIZE 0.125
    &END OT
    MAX_SCF_HISTORY 1
    SCF_GUESS HISTORY_RESTART
    &PRINT
    &RESTART_HISTORY
      EACH 1 1 0
      FILENAME =RESTART
      BACKUP_COPIES 5
    &END RESTART_HISTORY
    &END PRINT
  &END SCF
  &MD

```

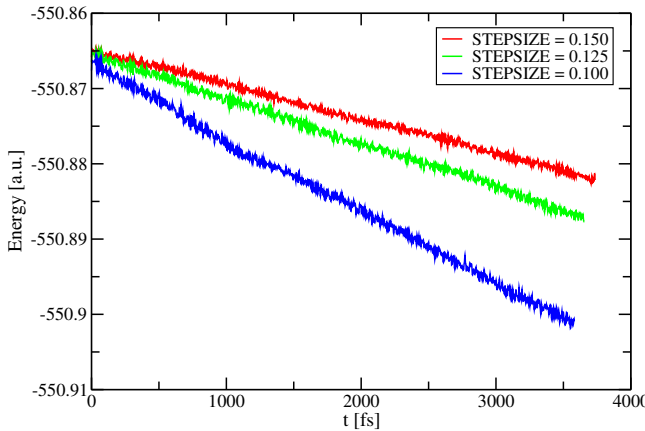


FIG. 2: Corrector step size determination

```

ENSEMBLE NVE
&END MD
&END DFT

```

We judge the quality of this parameter by monitoring the dissipation of total energy – less is better. Consulting Fig. (2), let us choose here STEPSIZE 0.15 and keep it fixed at this value.

B. Determination of the ASPC Propagation Order

It is apparent that the accuracy of our approximate eigenfunction depends only on the accuracy of the short-term integration of the electronic degrees of freedom. This is orthogonal to the integration of the ions, where the short-term accuracy is only of minor interest due to the Lyapunov instability. Therefore, we concluded that the integration of the ions and the electrons should not be treated on the same footing, even though it is treated as such in CPMD. We, therefore, decided to use the ASPC integrator instead, which is an explicit Gear-type predictor-corrector integrator for the integration of the electronic degrees of freedom.

Although ASPC is fairly good, it is not fully time-reversible but only time-reversible up to (and including) $\mathcal{O}(O^{K+2}) = \mathcal{O}(h^{k+4})$. To what extent this is important is an open question. Nevertheless, time-reversibility is assumed to be a desirable property, as the underlying Hamiltonian dynamics is time-reversible. A more severe issue is the fact that this particular integrator is not symplectic. Typically, explicit integrators are more accurate than implicit ones but are generally less likely to be symplectic.

The purpose of identifying the optimal order K is to minimize all aforementioned approximations by maximizing the time-reversibility as well as the integration accuracy. Typically, that coincides with the K that minimizes the dissipation. The procedure is therefore the same as in the previous subsection – the less energy dissipation, the better – but an eye should also

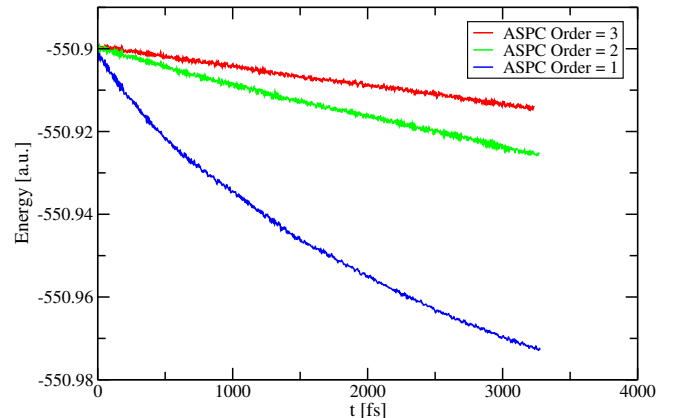


FIG. 3: Energy evolution with respect to the ASPC order

be kept on the OT convergence criterion. Lift different branches out from the relaxation run into separate folders and set STEPSIZE to the previously determined value. Vary EXTRAPOLATION_ORDER k by keeping all other parameters fixed. Usually, you will find the best EXTRAPOLATION_ORDER k somewhere between 0 and 3, causing time-reversibility up to $\mathcal{O}(h^4)$ and $\mathcal{O}(h^7)$, respectively. Disorder, smaller band gaps, higher temperatures, and larger integration time-steps h are all factors leading to a lower K value, which is preferred, though in our case, the input is the same as in the previous subsection.

As can be seen from Fig. (3), our initial guess of 3 is already the optimal value, so we keep everything as is and freeze this value from now on throughout the whole simulation.

IV. FINAL RELAXATION

With the previous steps, the accuracy of the DMP, and therefore the deviation from the BO surface is fixed. The energy dissipation is now well-minimized within the pre-defined number of corrector steps. As the deviation from the BO surface can be systematically controlled, it is the responsibility of the user to guarantee a sufficient accuracy and to test it if necessary. However, the required accuracy should not be exaggerated, because at the ab-initio level, it is normally superseded by single-particle finite-size effects and even more by statistical errors due to insufficient sampling, particularly in the presence of intrinsic correlation along any trajectory.

Alternatively, one can argue that there is not much physics involved in fully minimizing the energy functional, at least up to a constant shift in the energy. The main purpose is to minimize the residual non-self-consistent force²⁷, which is not explicitly calculated. In Car-Parrinello, this is solved in a very elegant manner by using an equation of motion (EOM) inspired by Ehrenfest dynamics²⁸ so that the instantaneous, rather than the fully minimized, expectation value of the Hamilto-

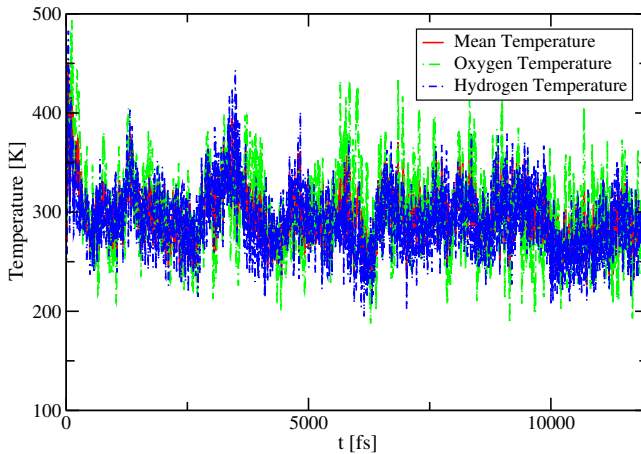


FIG. 4: Final Relaxation using the fast method

nian yields the consistent forces. In our new approach, a BO EOM without a fictitious mass is used, so we need to explicitly alleviate the non-self-consistent forces by minimizing them and rigorously correcting the remainder in terms of sampling.

As the Hamiltonian matrix is built up using the propagated density, it is now fully determined. If done correctly, it is very similar to the self-consistent KS Hamiltonian but is still different. It therefore needs to be explicitly relaxed, but now with the fast method. For this, our current input needs to be modified slightly by switching to ENSEMBLE LANGEVIN together with an appropriate noise, as in the first section.

```
&MD
ENSEMBLE LANGEVIN
GAMMA 0.01
&END MD
```

As I lifted this from the relaxation run while continuing it, contrary to Fig. (1), only the first 2.8 ps are BOMD relaxation, whereas the rest is relaxed in the manner just described. Once again, Fig. (4) indicates that proper equilibrium between the different atomic species is given and the difference in amplitude is only due to the stoichiometry.

V. PART II: TUNING THE MODIFIED LANGEVIN EQUATION TO ENSURE ACCURATE SAMPLING

The aim of this part is to correct our shortcomings in terms of sampling. As is well-known, a non-symplectic integrator turns a conservative system into a dissipative one due to phase-space compression, leading to an exponential decay in energy. Although no rigorous proof exists, this is, even from a mathematical perspective, “believed to be true”. We have verified that this is the case and that it suffices to simply adjust the mean temperature. Nevertheless, I will demonstrate that, by definition,

this should reduce to our original claim whenever the system is in equilibrium. In any case, explicitly checking the individual temperatures constitutes an additional and very hard test, which is much more sensitive than that for the mean temperature, and it is done to judge the proper adjustment of the γ values to be determined within this section.

In the process, we must abandon sampling the microcanonical for the physically more relevant canonical ensemble. Given a careful input design, this is no serious restriction as long as $\gamma = \gamma_D + \gamma_L$ is much lower than the typical inverse relaxation time of the particular system, because the dynamics are only marginally affected in such a case. Having specified the number of corrector steps and optimized the DMP, γ_D is now system-dependent and acts as a slider by which to control the aberration from the microcanonical ensemble, if this is of interest. It can be reduced to any desired degree by simply increasing the number of corrector steps. At the limit, this converges to BOMD, making time-reversibility and symplecticity of the integrator for the electronic degrees of freedom irrelevant, as the instantaneous ground state is distinct and independent of that. In this sense, it is analogous to the Car-Parrinello scheme, in which the fictitious mass acts as such a slider. However, the relationship between accuracy and speed is much more established, and it scales as $\sqrt{\mu}$ for both the maximum integration time step²⁹ and the deviation from the BO surface³⁰.

Nevertheless, one is typically interested in ensemble averages. In that case, the adjustments of the modified Langevin equation reduce to using a high GAMMA (γ_L) value and probably a sloppily determined NOISY_GAMMA (γ_D). A painstakingly accurate determination of NOISY_GAMMA is only needed when an approximation to the microcanonical ensemble is absolutely necessary.

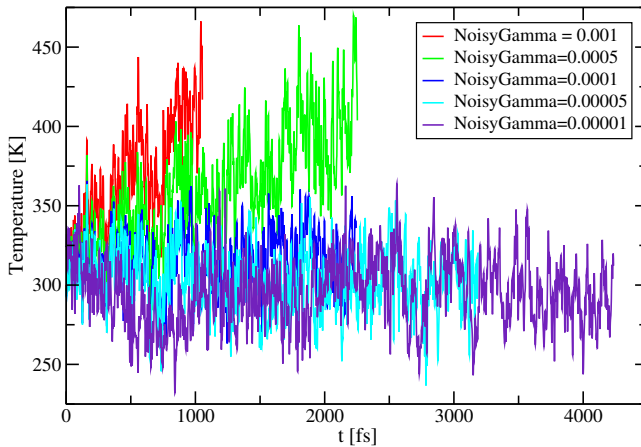
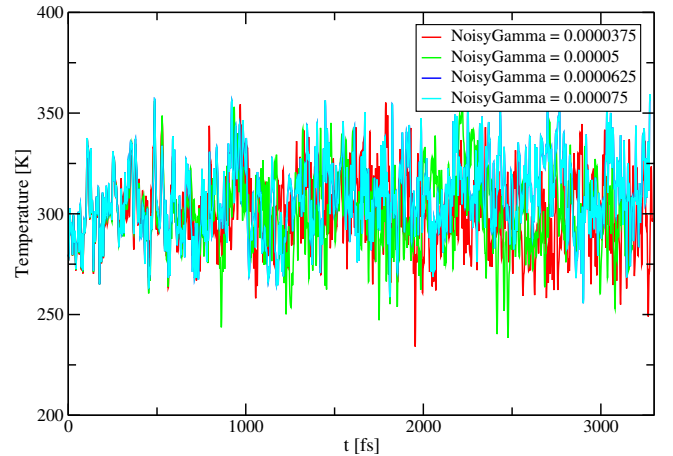
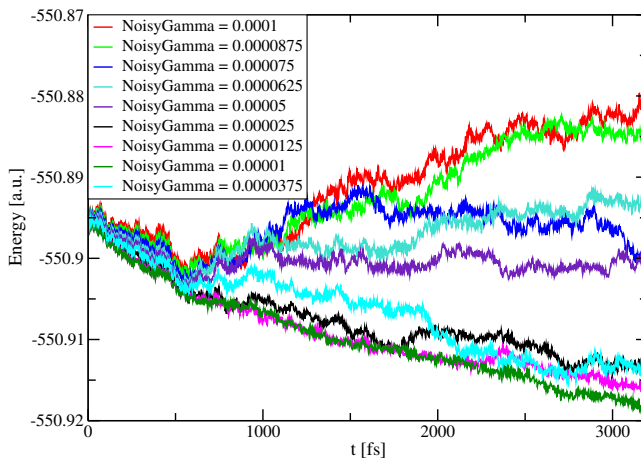
A. Determine γ_D by Bootstrapping

One can first start with a coarse-grained search to get an idea of what the final NOISY_GAMMA might look like. To do so, change the input to:

```
&MD
ENSEMBLE LANGEVIN
GAMMA 0.0
NOISY_GAMMA 0.0001
&END MD
```

To guess the initial range of γ_D values, it is advisable to orient oneself on the OT convergence criterion (preconditioned mean gradient deviation) of the final relaxation run using the fast method. The lower it is, the lower the “true” NOISY_GAMMA. Therefore, let us spread here 5 calculations within an initial range of $10^{-3} - 10^{-5}$.

Fig. (5), which shows the corresponding temperature evolution with time, clearly suggests that we can restrict

FIG. 5: Coarse-grained γ_D searchFIG. 7: Temperature evolution of the fine-grained γ_D searchFIG. 6: Energy evolution of the fine-grained γ_D search

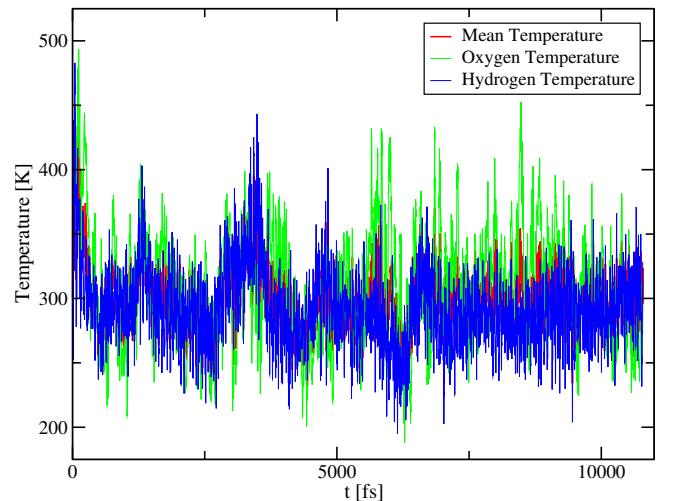
our fine-grained search to within $10^{-4} - 10^{-5}$. We therefore lift out of our in the meantime continued relaxation run using the fast method, 9 additional fine-grained runs equally distributed within the now reduced range (see Figs. (6) and (7)).

Here, we select `NOISY_GAMMA` 0.00005, and check our choice by observing the temperature evolution of the different atomic species (see Fig. (8)).

As one can see, they already agree fairly well. The remaining gap is attributed to the fact that we have bootstrapped the underlying “true” γ_D only within error bar. Therefore, a certain non-vanishing overlay noise γ_L may be necessary, depending on the accuracy of `NOISY_GAMMA`, and we actually recommend *always* using it.

B. Adding Overlay Noise to Ensure a Correct Sampling of the Boltzmann Distribution

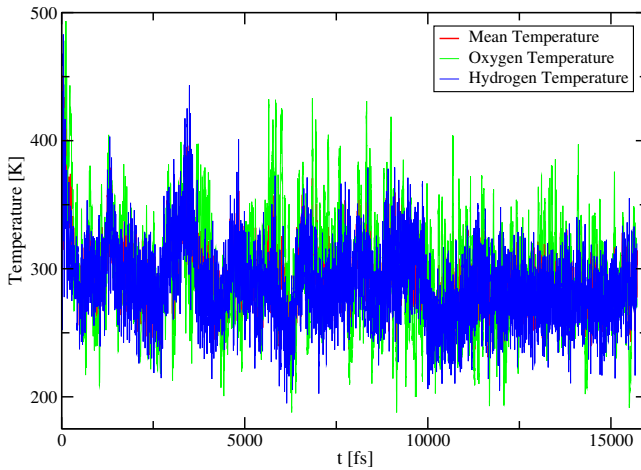
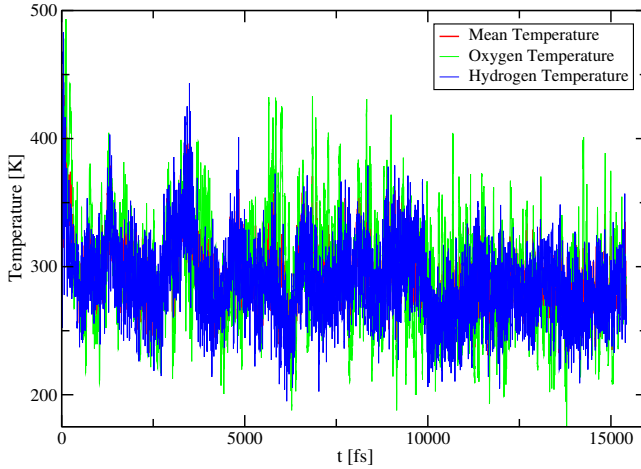
Here, we add both $\gamma_L = 10^{-4} \text{ fs}^{-1}$ and $\gamma_L = 3.75 \times 10^{-4} \text{ fs}^{-1}$. As can be seen from the results in Figs. (9) and (10), respectively, even the lower friction is sufficient

FIG. 8: Temperature evolution using $\gamma_D = 5 \times 10^{-5}$

to ensure the correct sampling and equilibrium desired between the involved atomic species. However, we advise to not be too frugal with γ_L and to explicitly check that the equilibrium between the atomic species is indeed achieved. It depends on the system, but in practice, even $\gamma > 10^{-4} \text{ fs}^{-1}$ have been used without any noticeable dynamical effect.

C. Atomic Species-Dependent Gamma Values

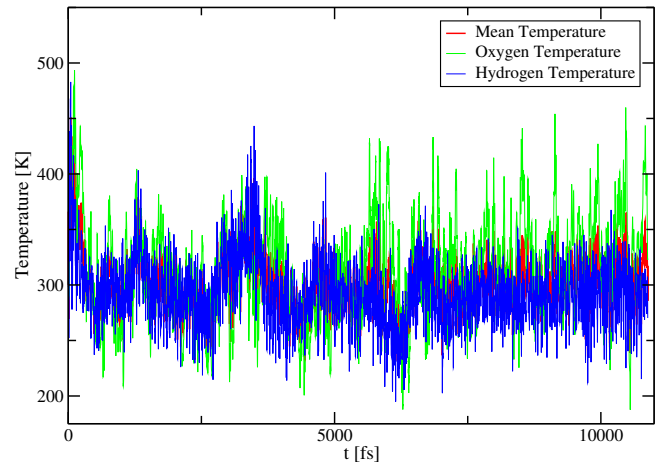
In summary, it appears that a proper input design, i.e. judicious control of the approximations through the number of corrector steps `MAX_SCF_HISTORY` together with a hence deduced `NOISY_GAMMA` in conjunction with sufficiently high γ_L , it should always be possible to perform a satisfying simulation, even with a global γ_D . Nevertheless, an additional mass dependence has recently been speculated, so one might therefore be interested in using atomic species-dependent γ_D values rather than a global

FIG. 9: $\gamma_L = 10^{-4}$ FIG. 10: $\gamma_L = 3.75 \times 10^{-4}$

one. For this, one can use `GAMMA_D` instead or in addition to `NOISY_GAMMA`. For instance, one can change the input as follows.

```
&MD
ENSEMBLE LANGEVIN
GAMMA 0.0
NOISY_GAMMA 0.00005000
GAMMA_D -0.00003125 0.00002500
&END MD
```

In that case, `GAMMA_D` acts as a correction to `NOISY_GAMMA`. However, even using solely `GAMMA_D` is possible, in which case the default 0 fs^{-1} would be assumed for `NOISY_GAMMA`. The list on the right hand side of `GAMMA_D` corresponds to the atomic species-dependent friction values for each atomic species involved, in order of occurrence in the `&COORD` section. In our case, $7.5 \times 10^{-5} \text{ fs}^{-1}$ is used for hydrogen and $1.875 \times 10^{-5} \text{ fs}^{-1}$ for oxygen in order to assess the conjecture $\gamma_D^I = \gamma_D \times \sqrt{\min_I M_I} / \sqrt{M_I}$. Unfortunately, it is not possible to entirely rule out this conjecture (see Fig. (11)). As a matter

FIG. 11: Species-dependent $\gamma_D^I = \gamma_D \times \sqrt{\min_I M_I} / \sqrt{M_I}$

of fact, even the original approach obeys the correct temperature distribution.

D. Concurrent Relaxation of nuclear and electronic degrees of freedom

Finally, by applying the following fragment, a so-called ‘‘Langevin annealing’’ can be performed, in which, inspired by the original Car-Parrinello approach, a damped Langevin dynamics is concurrently performed for the electronic and the nuclear degrees of freedom. In this way, structure relaxation, diagonalization and self-consistency are simultaneously achieved.

```
&MD
ENSEMBLE LANGEVIN
GAMMA 0.001
NOISY_GAMMA 0.00005
TEMPERATURE_ANNEALING 0.9999975
&END MD
```

If some kind of annealing, and not simply a quench, is actually performed, these are very expensive calculations, most likely enough to deplete the budget. We therefore have not explicitly performed an additional water annealing, but demonstrated this capability on an ab-initio annealing of liquid germania to vitreous germania (see Fig. (12)).

Acknowledgments

We would like to thank the whole CP2K team, in particular M. Krack, F. Mohamed, M. Iannuzzi and J. Hutter. The generous allocation of computer time from CSCS Manno and the ICT Services of ETH Zurich is acknowledged, as well as corresponding support from Neil Stringfellow and Olivier Byrde, respectively.

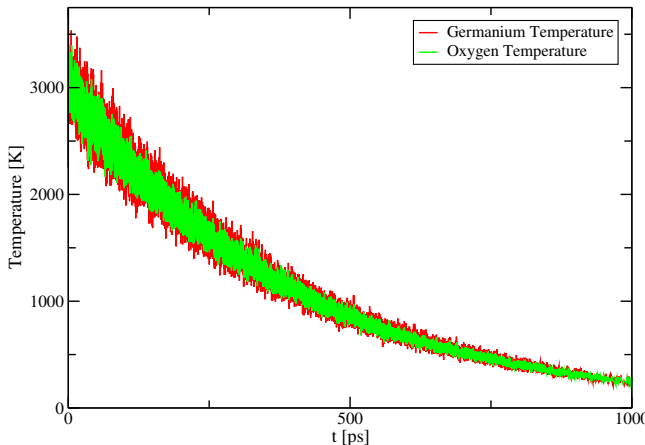


FIG. 12: Langevin annealing of liquid to vitreous germania

Appendix A: The applied GTH-PPs and Gaussian basis-sets

```

H GTH-PBE-q1
 1
 0.20000000 2 -4.17890044 0.72446331
 0
#
O GTH-PBE-q6
 2 4
 0.24455430 2 -16.66721480 2.48731132
 2
 0.22095592 1 18.33745811
 0.21133247 0

```

```

H DZVP-GTH
 2
 1 0 0 4 2
 8.3744350009 -0.0283380461 0.0000000000
 1.8058681460 -0.1333810052 0.0000000000
 0.4852528328 -0.3995676063 0.0000000000
 0.1658236932 -0.5531027541 1.0000000000
 2 1 1 1 1
 0.7270000000 1.0000000000
#
O DZVP-GTH
 2
 2 0 1 4 2 2
 8.85980961 0.13629371 0.00000000 -0.08866335 0.00000000
 2.79327113 0.02080784 0.00000000 -0.26937441 0.00000000
 0.90727943 -0.60919527 0.00000000 -0.45939673 0.00000000
 0.28741531 -0.50259053 1.00000000 -0.41039240 1.00000000
 3 2 2 1 1
 1.1850000000 1.0000000000

```

* Electronic address: tkuehne@cp2k.org

1 B. J. Alder and T. E. Wainwright, J. Chem. Phys. **27**, 1208 (1957).2 A. Rahman, Phys. Rev. **136**, A 405 (1964).3 T. D. Kühne, M. Krack, F. Mohamed and M. Parrinello, Phys. Rev. Lett. **98**, 066401 (2007).4 T. D. Kühne, WIREs Comput. Mol. Sci. **4**, 391 (2014).5 T. D. Kühne and E. Prodan, Annals of Physics **391**, 120 (2018).6 P. Hohenberg and W. Kohn, Phys. Rev. **136**, B864 (1964).7 W. Kohn and L. J. Sham, Phys. Rev. **140**, A1133 (1965).8 M. C. Payne, M. P. Teter, D. C. Allan, T. A. Arias and J. D. Joannopoulos, Rev. Mod. Phys. **64**, 1045 (1992).9 S. Nosé, Mol. Phys. **52**, 255 (1984).10 W. Hoover, Phys. Rev. A **31**, 1695 (1985).11 A. Ricci and G. Ciccotti, Mol. Phys. **101**, 1927 (2003).12 G. Bussi, D. Donadio and M. Parrinello, J. Chem. Phys. **126**, 014101 (2007).13 T. D. Kühne et al., J. Chem. Phys. **152**, 194103 (2020).14 T. D. Kühne, M. Krack and M. Parrinello, J. Chem. Theory Comput. **5**, 235 (2009).15 M. W. Mahoney and W. L. Jorgensen, J. Chem. Phys. **112**, 8910 (2000).16 S. Goedecker, M. Teter and J. Hutter, Phys. Rev. B **54**, 1703 (1996).17 C. Hartwigsen, S. Goedecker and J. Hutter, Phys. Rev. B **58**, 3641 (1998).18 M. Krack, Theor. Chem. Acc. **114**, 145 (2005).19 J. Kolafa, J. Comput. Chem. **25**, 335 (2004).20 J. Kolafa, J. Chem. Phys. **122**, 164105 (2005).

²¹ A. Edelman, T. A. Arias and S. T. Smith, SIAM J. Matrix Anal. Appl. **20**, 303 (1998).

²² R. Car and M. Parrinello, Phys. Rev. Lett. **55**, 2471 (1985).

²³ J. VandeVondele and J. Hutter, J. Chem. Phys. **118**, 4365 (2003).

²⁴ J. Hutter, M. Parrinello and S. Vogel, J. Chem. Phys. **101**, 3862 (1994).

²⁵ C. K. Gan, P. D. Haynes and M. C. Payne, Comput. Phys. Commun. **134**, 33 (2001).

²⁶ C. W. Gear, *Numerical Initial Value Problems in Ordinary Differential Equations* (Prentice-Hall, Englewood Cliffs, NJ, 1971).

²⁷ D. Marx and J. Hutter, FZ Jülich, NIC Series **1**, 301 (2000).

²⁸ P. Ehrenfest, Z. Phys. **45**, 455 (1927).

²⁹ G. Pastore, E. Smargiassi and F. Buda, Phys. Rev. A **44**, 6334 (1991).

³⁰ F. A. Bornemann and C. Schütte, Numer. Math. **78**, 359 (1998).